Arabian Journal of Geosciences (2018) 11: 147
https://doi.org/10.1007/s12517-018-3500-z

ORIGINAL PAPER

Provenance, weathering, and paleoenvironment of the Upper Cretaceous Duwi black shales, Aswan Governorate, Egypt

Samir M. Zaid[1] · Oussama A. EL-Badry[1] · Adel M. Akarish[2] · Mahmoud A. Mohamed[1]

Received: 6 October 2017 / Accepted: 15 March 2018 / Published online: 2 April 2018
© Saudi Society for Geosciences 2018

Abstract

The mineralogy and geochemistry of the Upper Cretaceous Duwi black shales of Nile Valley district, Aswan Governorate, Egypt, have been investigated to identify the source rock characteristics, paleoweathering, and paleoenvironment of the source area. The Duwi Formation consists mainly of phosphorite and black shales and is subdivided into three members. The lower and upper members composed mainly of phosphorite beds intercalated with thin lenses of gray shales, while the middle member is mainly composed of gray shale, cracked, and filled with gypsum. Mineralogically, the Duwi black shales consist mainly of smectite and kaolinite. The non-clay minerals are dominated by quartz, calcite, phosphate, dolomite, feldspar, with little gypsum, anhydrite, iron oxides, and pyrite. Based on the CIA, PIA, and CIW values (average = 84, 94, 95, respectively), it can be concluded that the litho-components of the studied shales were subjected to intense chemical weathering and reflect warm/humid climatic conditions in the depositional basin. The provenance discrimination diagram indicates that the nature of the source rocks probably was mainly intermediate and mafic igneous sources with subordinate recycled sedimentary rocks (Nubia Formation). Geochemical characteristics indicate that the Duwi black shales in Nile Valley district were deposited under anoxic reducing marine environments.

Keywords Provenance · Black shales · Upper Cretaceous · Aswan

Introduction

The black shales have attracted the interest of many researchers primarily because of their economic importance in terms of hydrocarbon development potential (i.e., source rocks) as well as metal concentrations (Wignall 1993; El Kammar 1993; Armstrong-Altrin et al. 2013). Several black shales are particularly metalliferous, mostly enriched in U, V, Cu, Ni, and Zn (Schultz 1991). The black shale could be used also as an energy donator in an electric power plant and/or in production of cement. The composition of the inorganic fraction may vary from a shale where clay minerals are predominant, to carbonates with subordinate amounts of clay and other minerals. The organic fraction is mainly an insoluble solid material (kerogen) which is entirely comparable to the organic matter present in many petroleum source rocks. The abundance of organic rich layers was confirmed in place because parts of the Duwi mine are still burning after they caught fire some years ago. The organic matter is derived from dominating marine organisms under strong reducing conditions (El Kammar et al. 1990; El Kammar 1993).

The black shales in Egypt belong to two stratigraphic formations namely Duwi at the base overlain by the Dakhla of Campanian–Maastrichtian age. Both formations persistently extend along the southern escarpments which bound the Western Desert from Dakhla to Kharga Oasis, to south Kharga at Sinn El-Kaddab escarpment, further to the western reaches of Kom-Ombo, then traced northward along the Nile Valley from Idfu to wadi Qena and the Galala plateau, as well as along the Red Sea Coast between Quseir and Safaga forming a thick belt.

Black shales are argillaceous sediments containing high percent of total organic carbon. Their depositional controls are not clear, but are widely viewed as a complex interplay between surface water productivity, rates of oxidation of

✉ Samir M. Zaid
Samir_zaid75@yahoo.com

[1] Department of Geology, Faculty of Sciences, Zagazig University, Zagazig, Egypt

[2] Department of Geological Sciences, National Research Centre, Dokki, Giza, Egypt

organic matter, and/or dilution by non-organic material (Bottcher et al. 2006). The mineralogy and chemistry of black shales have been affected, therefore by numerous factors including composition of source material, duration of weathering, transportation mechanisms, bulk sediment accumulation rate, prevailing organisms, chemical composition of water, and diagenesis (Loukola-Ruskeeniemi 1991; Hayashi et al. 1997; Armstrong-Altrin et al. 2004, 2013). Shales that are the most abundant type of detrital sediments in sedimentary basins (Pettijohn 1975) are represented by the average crustal composition of the provenance area much better than any other siliciclastic sedimentary rocks (Nagarajan et al. 2007), since they preserve the original signature of the source rocks and diagenetic history (Mondal et al. 2012). Chemical composition of the clastic sediments provides important information on provenance, weathering conditions, and sediment recycling (Basu et al. 2016; Borghesi et al. 2016; Campodonico et al. 2016; Selvaraj et al. 2016; Tawfik et al. 2016; Tobia and Shangola 2016; Armstrong-Altrin et al. 2015a, b). Also, the geochemical parameters have been used by various authors to interpret the paleoenvironment and paleooxygenation conditions of ancient shales (Nagarajan et al. 2007; Abou El-Anwar et al. 2017).

Significant contributions have been made by several studies in relation to the regional geology, sedimentology, mineralogy, geochemistry, and economic potentiality of the Upper Cretaceous Duwi black shales exposed at Western Desert district, Nile Valley district, and the Red Sea coastal zone (Sediek and Amer 2001; Ghandour et al. 2003; Ibrahim et al. 2004; Schulte et al. 2011, 2013; El Kammar 2014; Ghanem et al. 2016; Abou El-Anwar and Gomaa 2016; Abou El-Anwar et al. 2017). In contrast, no detailed studies that focused on provenance, paleoweathering, and paleoenvironments of the Upper Cretaceous Duwi black shales have been documented. Therefore, the present work aims to examine the mineralogy and geochemistry of the Upper Cretaceous Duwi black shales at five sites at El-Nasr company open-pit exploited phosphate mines, Nile Valley district (Kom-Mir, El Sebaiya, Um Salamah, Badr-3, Elgididh-6, Figs. 1 and 2) in Aswan Governorate, Egypt, to identify the source rock characteristics, palaeoweathering, and paleoenvironment of the source area.

Geological setting

The study area lies between longitudes 32° 30′–32° 50′ E and latitudes 25° 05′–25° 30′ N, on the southwestern side of the Nile Valley (Fig. 1). The stratigraphic succession is of Late Campanian–Early Paleocene age and represents a part of the dominated sedimentary deposits of black and variegated shales that are widely distributed in Upper Egypt. This succession laterally extends from the New Valley in the Western Desert to Safaga–El Qusier region on the Red Sea Coastal plain through Aswan at Nile Valley. The study area contains occurrences of extensive black shale beds of Duwi Formation (Late Campanian–Early Maastrichtian) that overlie a fluvial variegated shale sequence in Quseir member of the older Nubia Formation, with an undulating erosion contact (El-Azabi and Farouk 2010). The entire succession is conformably overlained by the deeper marine laminated gray to black shales of the Dakhla Formation (Late Maastrichtian–Early Paleocene) (Fig. 2).

The Quseir shale member is composed of different variegated shales, reddish brown, gray, and yellow in color. The Duwi Formation composes of a lower phosphorite member represented by phosphorite bed intercalated with thin lenses of gray shales of thickness ranging between 0.2 and 0.6 m averaging 0.4 m, and the middle shale member is mainly composed of gray shale, cracked, and filled with gypsum. Meanwhile, the Upper Phosphorite Member is composed of thin phosphatic beds. The Dakhla Formation is composed of gray to black shale, papery, cracked, and filled with gypsum and ferruginous stains. Obviously, the deposition represents an initial stage of the Late Cretaceous marine transgression in Egypt (Glenn and Arthur 1990; El-Azabi and Farouk 2010).

The northwestern margin of the Red Sea consists of Precambrian crystalline basement together with Mesozoic, Cenozoic pre-rift sediment, and the late Oligocene–Miocene to recent syn-rift sediments (Said 1990). The pre-rifting (Late Cretaceous–Middle Eocene) deposits of a 500–700 m thick occupy the troughs of synformal-like folds within the basement hill ranges. The lower part of the pre-rift section is the 130-m massive thick-bedded siliciclastic Nubia Formation which overlain by 220–370-m-thick sequence of interbedded shales, sandstones, and limestones of Quseir, Duwi, Dakhla, and Esna formations (Khalil and McClay 2009). The uppermost pre-rift strata consists of 130–200 m of competent, thick-bedded limestones and cherty limestone of the lower to middle Eocene Thebes Formation. The marine upper Eocene and Oligocene deposits are absent, indicating that the region must have undergone elevation changes during these two epochs (Said 1992). The late Oligocene to recent syn-rift strata unconformably overlie Thebes Formation and vary in thickness from less than 100 m on shore to as much a 5 km in offshore basin (Heath et al. 1998). Faulting with a dominant NW trend is the main feature in the region and forms complicated horsts and grabens with outcropping basement rocks covering the major part of this region.

Samples and methodology

Twenty-five representative samples of Duwi black shale were collected from the Duwi phosphate mines belonging to El Nasr mining company namely Kom-Mir, El Sebaiya, Um

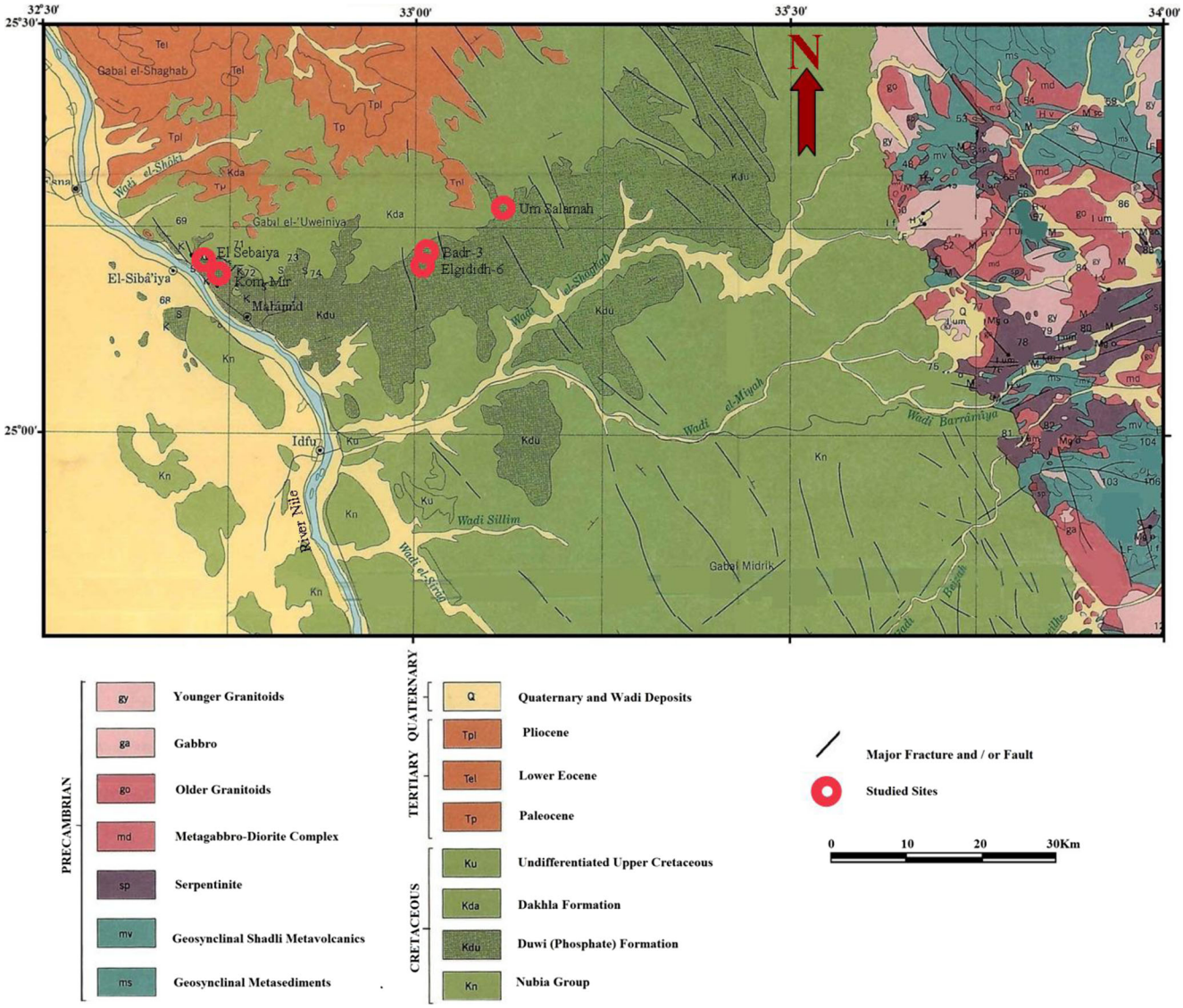

Fig. 1 Geological map of the study area showing locations of studied sites (modified after Conoco 1987)

Salamah, Badr-3, and Elgididh in Aswan Governorate, Nile Valley district (Fig. 1). The petrographic characteristics of 10 selected samples were investigated by thin section microscopic observations. The mineralogy of all Duwi black shale samples was determined by X-ray diffraction (XRD) analysis using both smear-on glass slide and powder press techniques (Hardy and Tucker 1988). The analysis was done by a Philips X-ray diffractometer model PW/1710 (CuKα radiation with 40 kV, 35 mA, and 2°–70° 2-theta). Clay minerals were identified by their characteristic reflections (Moore and Reynolds Jr 1997). Also, the samples were scanned by scanning electronic microscope (SEM, 3.5 nm of resolution) equipped with energy-dispersive spectrometer (EDS), to determine the chemical composition during SEM observations. XRD and SEM-EDS analyses were performed at the laboratory of the Central Metallurgical Research and Development Institute, Egypt.

Twenty-five shale samples were grinded to < 63 μm and dried at 110 °C and treated with lithium metaborate and tetraborate to make pressed powder pellets. They were analyzed using X-ray fluorescence Pnalytical Axios Advanced XRF equipment for major and trace element geochemistry. XRF analyses were performed at the laboratory of the Central Metallurgical Research and Development Institute, Egypt. The accuracy of the analytical method was evaluated using the standard MESS-3 and was $100 \pm 3\%$ for all oxides and trace elements. Loss on ignition (LOI) was estimated by heating sample at 1000 °C for 2 h. Major element data were recalculated to an anhydrous (LOI-free) basis and adjusted to 100% before using them in various diagrams. The total iron is expressed as Fe_2O_3. The correlation coefficient has been carried out for the chemical data by using the Davis method (1986).

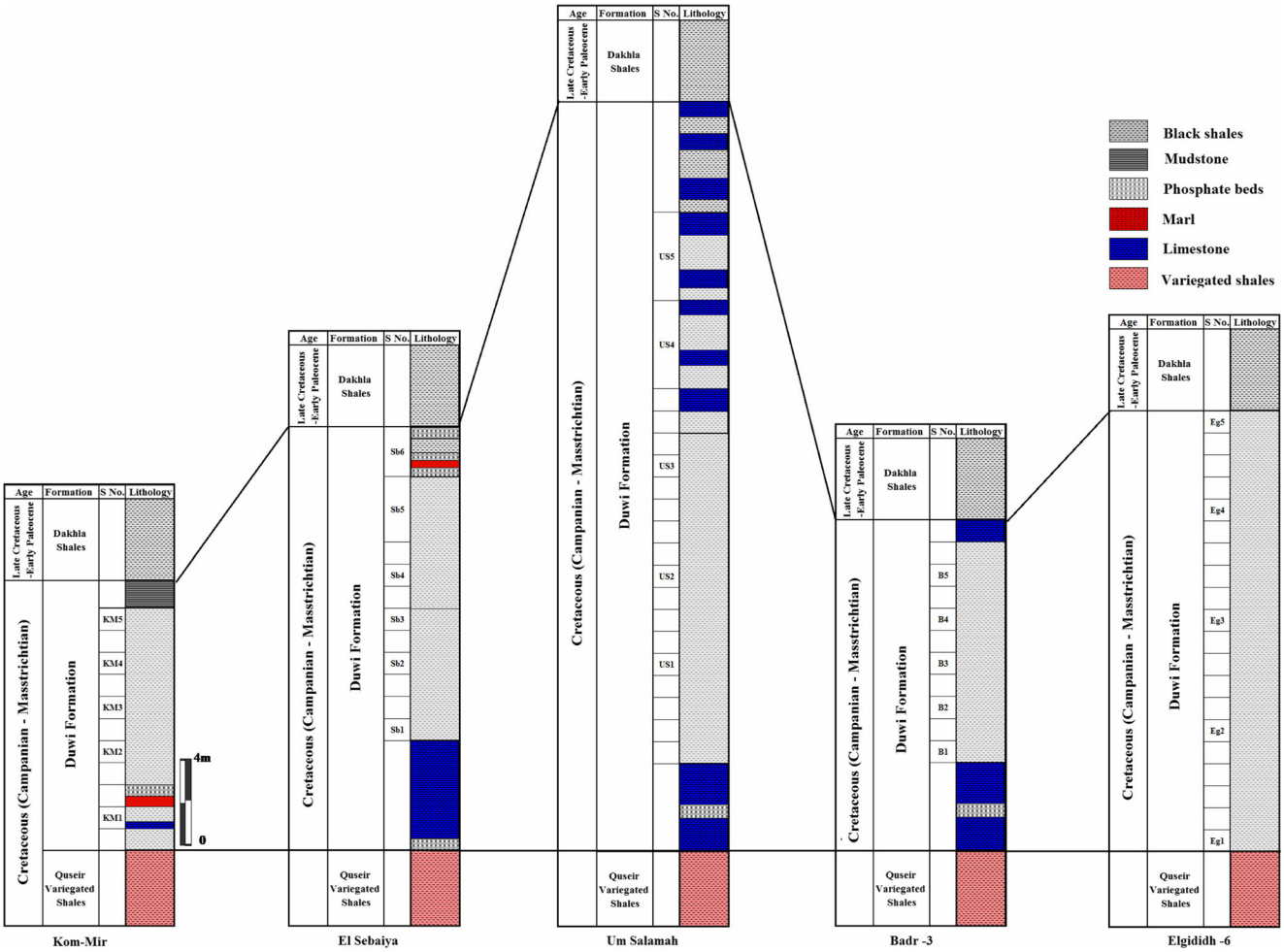

Fig. 2 Correlation chart of the Duwi Formation at the studied locations: (1) Kom-Mir, (2) El Sebaiya, (3) Um Salamah, (4) Badr-3, and (5) Elgididh-6, Aswan Governorate, Egypt

Results

Petrography

The shales consist mainly of foraminiferal argillaceous matrix (Fig. 3a). In some samples, the argillaceous matrix is color-laminated (Fig. 3b). This lamination resulted from the alteration of organic matter-rich and iron oxide-rich laminae. Sand-sized grains (average 31%, Table 1) are embedded in argillaceous materials (Fig. 3c, d). Quartz grains are generally fine to very fine, angular to subangular, monocrystalline, poorly sorted, and exhibit either uniform or undulose extinction (Fig. 3c, d). Feldspars (average 4%, Table 1) are represented mainly by Na-plagioclase (albite) and K-feldspar (microcline). Iron oxides (average 1%, Table 1), are formed of very fine material or dark patches replacing the clay matrix (Fig. 3e). This indicates that these iron oxides are authigenic and were either precipitated by moving fluids or resulted by the degradation and breakdown of iron-rich minerals and detrital ferromagnesian silicates.

Mineralogy

The XRD results indicate that the Upper Cretaceous Duwi black shales consist mainly of quartz, calcite, smectite and kaolinite clay minerals, phosphate, dolomite, feldspar, with little gypsum, anhydrite, iron oxides, and pyrite (Table 1; Fig. 4). Iron oxides (mainly hematite) are recorded in Sebaiya, Badr-3, and Elgididh-6 black shales (Table 1). It increases from east to west. Smectite and kaolinite (average = 20.48%) constitutes the most abundant clay minerals. Their values increase from the west (Badr-3, Elgididh-6, and Um Salamah) to the east (Sebaiya). The bulk rock mineralogy of the shales indicates the presence of phyllosilicates with abundant quartz, calcite, phosphate (fluorapatite), dolomite, and feldspar. Quartz is the most abundant non-clay minerals (average = 31%) followed by calcite (average = 20.9%), fluorapatite (average = 10.4%), dolomite (average = 6.9%), feldspar (average = 4%), gypsum (up to 3.5%), anhydrite (up to 1.5%), iron oxide, and pyrite (up to 1.5%). The mineralogical composition indicates a high MMI (mudrock maturity

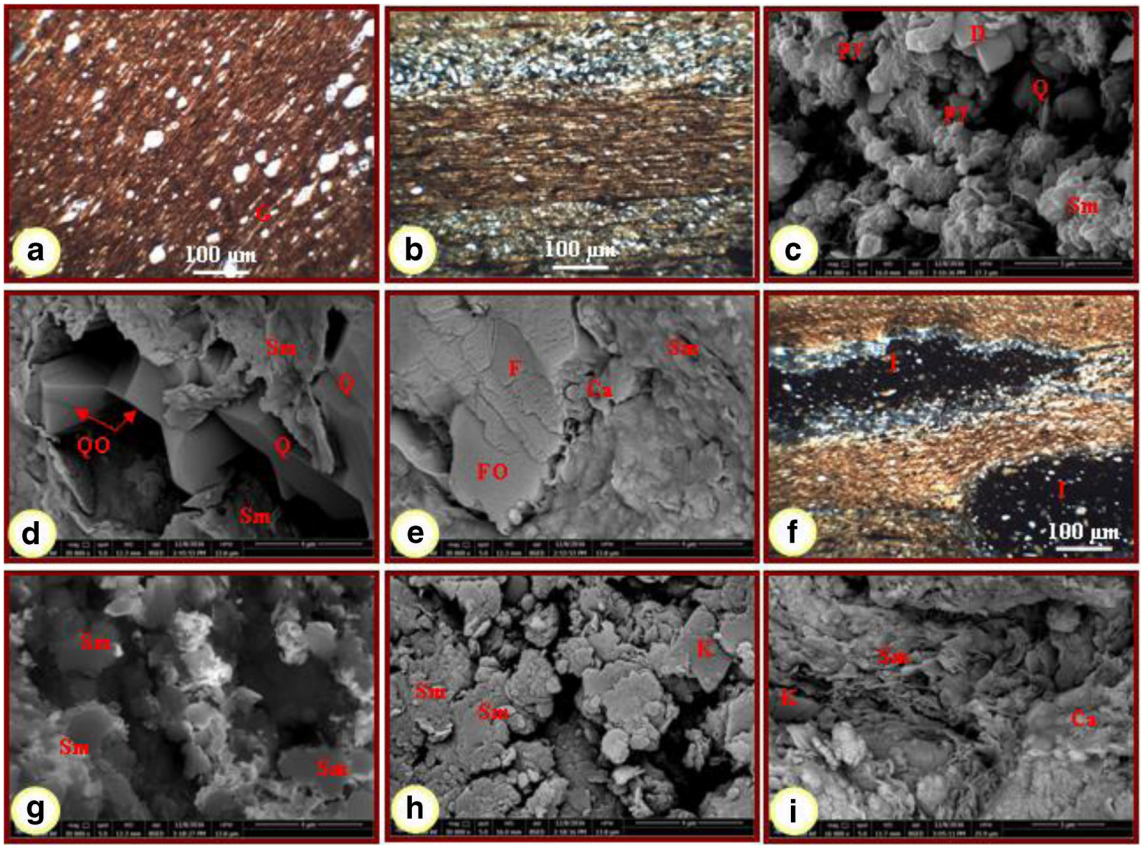

Fig. 3 Photomicrograph and SEM of the Duwi black shales showing **a** highly foraminiferal argillaceous matrix with thin bands of gypsum/anhydrite (G), a laminated foraminiferal shale (note minor scattered silt-sized quartz grains (Q) in argillaceous matrix); **b** fine to very fine quartz grain (Q) embedded in argillaceous matrix (note rhombic dolomite crystals (D) and aggregates of framboidal pyrite (Py); **c** quartz grains (Q) embedded in argillaceous matrix (note pore-filling euhedral pyramidal syntaxial overgrowth (QO); **d** feldspar grains embedded in calcite (Ca) cement and argillaceous matrix (note feldspar overgrowth (FO)); **e** argillaceous matrix are partially replaced by iron oxides (I); **f** detrital particles of smectite (Sm); **g** detrital platelets of kaolinite (K) (note irregular edges of smectite (Sm); and **h** detrital particles of smectite (Sm) and kaolinite (K) embedded in calcite (Ca) cement

index; MMI = 100 × phyllosilicates / (phyllosilicates + quartz + feldspars; Bhatia 1985), with an average value of 36 (Table 1).

Clay minerals

Smectite (Fig. 3c–e, g–i) constitute the dominant clay mineral content of the studied shale samples. It ranges from 0.8 to 63.7% (Table 1). The abundance of smectite, the low content of kaolinite, the presence of pyrite rhombs, and the complete absence of illite in the shales refer to a deposition under fluvio-marine environment under alkaline-reducing conditions (Sediek and Amer 2001). Also, the absence of any volcanic precursor, such as tuff or glass in the studied shales, proves that smectite is mainly of detrital origin. Generally, the clay mineral associations in the studied shales with its smectite dominance and low kaolinite suggest a terrestrial provenance that are degraded from chlorite and illite after deposition and had not attained intensive weathering, under a warm and semi-arid climate, and the resulted materials were carried by fluvial action, which finally interfered and admixed with marine environments (marginal marine, low energy, and reducing conditions of Duwi Formation) (Hendriks et al. 1990).

Kaolinite (Fig. 3h, i) constitutes the second dominant clay mineral in the studied black shale of Duwi Formation. It ranges from 0.2 to 1.3% (Table 1). Kaolinite in the marine deposits of Upper Cretaceous age are products of terrestrial weathering and represent continental products of a warm and at least seasonally humid climate, being eroded and transported toward the sea by rivers (Hendriks et al. 1990; Hallam et al. 1991). In addition to a detrital origin, smectite and kaolinite may also develop by diagenetic processes due to the circulation of acid solutions (Ghandour et al. 2003).

Non-clay minerals

Quartz (avg. = 31%, Table 1) was present as an important non-clay mineral in shales. Quartz grains (Fig. 3c, d) are fine to

Table 1 Semi-quantitative mineralogical composition of bulk studied samples

Location	Kom-Mir					El Sebaiya					Um Salamah					Badr-3					Elgidiidh-6					Statistical parameters		
	KM1	KM2	KM3	KM4	KM5	Sb1	Sb2	Sb3	Sb4	Sb5	US1	US2	US3	US4	US5	B1	B2	B3	B4	B5	Eg1	Eg2	Eg3	Eg4	Eg5	Av	Min	Max
Quartz	39	5	17	4	17	33	44	53	41	63	64	63	32	15	47	1	14	43	27	18	29	30	19	9	50	31.1	1	64
Feldspar	0	0	0	0	0	4	10	30	15	5	19	14	0	0	0	0	0	0	0	0	0	0	0	0	4	4.0	0	30
Calcite	14	94	4	0	0	0	0	0	0	0	0	0	0	50	13	0	52	0	54	61	56	56	68	0	0	20.9	0	94
Dolomite	0	0	0	76	46	0	0	0	0	0	0	0	0	0	0	0	0	0	0	0	0	0	0	50	0	6.9	0	76
Anhydrite	0	0	0	0	0	10	11	0	13	0	0	0	0	0	0	0	0	0	0	0	0	0	0	0	0	1.4	0	13
F-apatite	45	0	69	0	0	0	0	0	0	0	0	0	0	30	14	52	0	0	10	0	0	0	0	40	0	10.4	0	69
Iron oxides	0	0	0	0	0	15	0	0	0	0	0	0	0	0	0	0	0	0	0	8	0	0	0	0	5	1.1	0	15
Gypsum	0	0	0	2	0	1	0	0	0	0	0	0	1	0	0	45	33	4	0	0	0	0	0	0	0	3.4	0	45
Pyrite	0	0	0	0	0	0	0	0	0	0	0	1	2	0	0	0	0	4	0	0	0	0	1	0	0	0.32	0	4
Clay minerals	2	1	10	18	37	37	35	17	31	32	17	22	65	5	26	2	1	49	9	13	15	14	12	1	41	20.5	1	65
MMI	4.9	16.7	37.0	81.8	68.5	50.0	39.3	17.0	35.6	32.0	17.0	22.2	67.0	25.0	35.6	66.7	6.7	53.3	25.0	41.9	34.1	31.8	38.7	10.0	43.2	36.0	4.87	81.8
< 2 μm clay Sm	86	87	87	81	88	89	85	92	86	97	95	98	91	86	94	93	92	97	93	95	94	91	93	94	92	91.0	81	98
K	14	13	13	19	12	11	15	8	14	3	5	2	9	14	6	7	8	3	7	5	6	9	7	6	8	8.9	2	19

MMI = 100 × phyllosilicates / (phyllosilicates + quartz + feldspars) (Bhatia 1985)

Av average, *Min* minimum, *Max* maximum, *MMI* mudrock maturity index

very fine grained, angular to subangular, mostly monocrystalline, with normal and undulose extinction.

Carbonate minerals detected are calcite and dolomite. Calcite (Fig. 3e, i) was recorded in all studied sites except El Sebaiya (Table 1). It ranges from 0.0% to about 94%. On the other hand, dolomite (Fig. 3c) was recorded only in shales of Kom-Mir and Elgididh-6 phosphate mines. It reaches up to 76% (Table 1). The presence of calcite and dolomite in shales in addition to the presence of foraminifers' fossils may indicate the deposition of this formation in a marine environment.

Sulfates detected by XRD are gypsum and anhydrite (Table 1 and Fig. 3a). Anhydrite was found only in El Sebaiya black shale, while gypsum was recorded in all studied sites except Elgididh-6 black shale. The anhydrite content reaches up to 13%, while gypsum content reaches up to 45%. The evaporites form from saline-rich fluids-brines. Brines may be generated by concentration of sea water, by evaporation or freezing, or as residual connate fluids in the subsurface (Selley 1988).

Anhydrite and gypsum was probably syn-precipitated under reducing conditions primarily as sulfides with shale. After shale compaction, the sulfides oxidized to sulfates as a result of biogenic activity; the sulfates react with the calcic cement (produced by weathering of carbonate) to form gypsum. Due to the compaction of clays, the sulfates will be expelled and concentrated along the bedding planes as gypsiferous bands which can be seen in the field.

Phosphate minerals encountered in Duwi black shales are carbonate fluorapatite (francolite). It is recorded in all studied sites except El Sebaiya. It varies from 0 to 69% (Table 1). The carbonate and phosphate minerals, in the shales, are indicating their deposition in a marine environment (Temraz 2005).

Feldspars detected by XRD are represented mainly by Na-plagioclase (albite) and K-feldspar (microcline) in the shales (Fig. 4). It varies from 0 to 30% (Table 1). Microcline is relatively more common than plagioclase. The absence of feldspar in most samples may indicate intensive degree of chemical weathering.

Iron oxides detected by XRD in Duwi black shale samples are represented mainly by hematite (Fig. 4). The hematite content reaches up to 15% (Table 1). It is commonly present as very fine material replacing the clay matrix or as dark patches (Fig. 3f). Iron oxides can be formed either by pedogenic processes or by the precipitation of iron oxides from laterally flowing surface or groundwater (Ollier and Galloway 1990).

Pyrite spheres and framboids were recorded in most samples of the Duwi Formation except El Sebaiya black shale (Table 1 and Fig. 3c). It is recorded only in Um Salamah, Badr-3, and Elgididh-6. The pyrite content reaches up to 4%

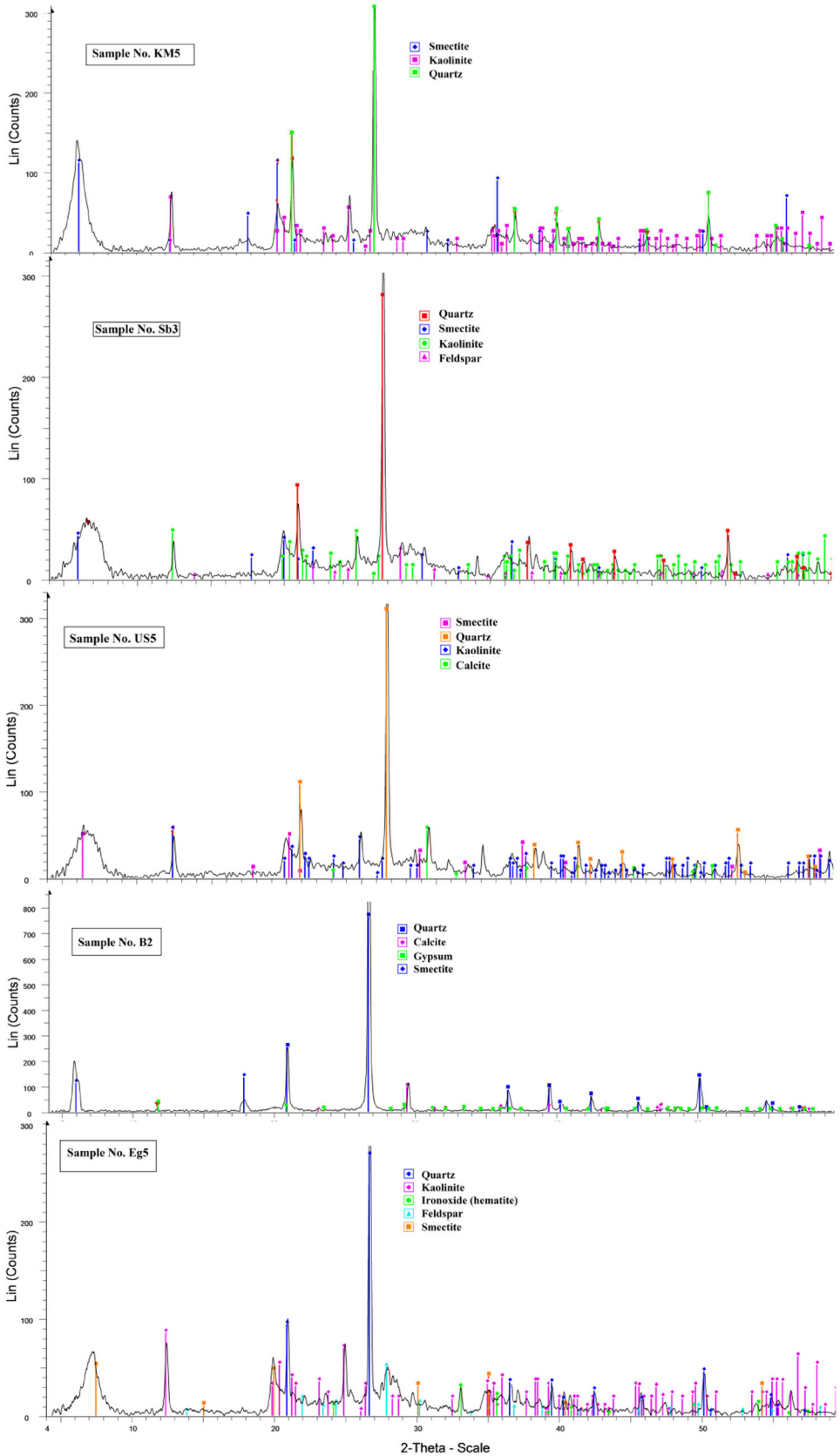

Fig. 4 X-ray diffraction patterns of the Duwi black shale samples at (1) Kom-Mir (sample KM5), (2) El Sebaiya (sample Sb3), (3) Um Salamah (sample US5), (4) Badr-3 (sample B2), and (5) Elgididh-6 (sample Eg5), Aswan Governorate, Egypt

Table 2 Major element composition (wt%) of Duwi black shales, Aswan Governorate, Egypt

Location	Kom-Mir					El Sebaiya					Um Salamah					Badr-3					Elgididh-6					Av	Std
	KM1	KM2	KM3	KM4	KM5	Sb1	Sb2	Sb3	Sb4	Sb5	US1	US2	US3	US4	US5	B1	B2	B3	B4	B5	Eg1	Eg2	Eg3	Eg4	Eg5		
$(SiO_2)_{adj}$	52.99	52.65	54.80	53.36	55.31	52.25	52.13	54.15	54.25	53.69	54.46	52.44	53.91	54.39	54.02	53.55	51.85	52.75	55.55	55.70	51.08	52.01	53.95	54.02	52.83	53.47	1.43
SiO_2	43.1	43.3	44.2	42.4	45.4	41.41	43.2	42.5	44.5	42.02	45.1	41.55	42.7	42.27	42.30	41.80	40.3	40.9	43.5	42.7	40.38	40.62	42.30	41.80	41.40	41.69	1.00
Al_2O_3	12.8	12.9	13.8	13.1	13.2	13.9	14.8	12.7	13.91	12.8	13.3	14.3	13.4	12.10	12.30	12.96	11.3	11.7	13.07	11.81	12.7	11.6	12.20	11.80	11.90	12.12	0.55
CaO	5.8	6.3	5.1	4.1	4.2	4.5	5.3	4.1	4.9	4.2	5.3	4.6	4.4	5.40	5.30	5.40	7.3	8.1	4.3	4.5	6.4	6.3	5.63	6.00	6.00	5.89	1.07
MgO	1.6	1.2	1.4	1.3	1.9	1.3	1.4	1.1	1.3	1.5	1.3	1.1	1.5	1.60	1.57	1.58	1.7	1.4	1.4	1.7	1.6	1.7	1.56	1.56	1.58	1.58	0.10
Fe_2O_3*	11.1	11.1	9.2	12.1	11.3	12.2	12	11.7	11.6	11.6	11.7	12.5	11.4	10.80	11.20	10.48	10.9	9.9	10.8	10.8	11.4	11.7	11.00	10.70	11.50	10.93	0.48
TiO_2	0.9	1.3	0.9	1.1	1	1	0.9	0.91	1.1	1	0.96	0.45	0.27	0.57	0.55	0.56	0.4	0.4	0.7	0.6	0.5	0.4	0.55	0.53	0.54	0.53	0.09
P_2O_5	3.3	3.1	3.3	2.5	2.1	2.1	2	2.9	2.2	2.6	2.5	2.2	3.2	2.70	2.80	2.86	3.3	2.6	2.3	2.5	3.2	3.4	2.80	2.65	2.90	2.83	0.33
Na_2O	0.9	0.9	0.8	0.8	0.9	0.88	1.1	0.8	0.86	0.8	0.8	0.8	0.7	0.60	0.60	0.66	0.7	0.7	0.6	0.5	0.8	0.6	0.63	0.62	0.70	0.64	0.08
K_2O	1.7	2	1.8	1.9	1.9	1.8	2	1.6	1.5	1.6	1.7	1.6	1.5	1.53	1.54	1.60	1.7	1.7	1.5	1.4	1.9	1.6	1.59	1.57	1.70	1.61	0.13
SO_3	0.14	0.14	0.15	0.16	0.19	0.17	0.17	0.17	0.16	0.14	0.15	0.13	0.14	0.14	0.15	0.16	0.13	0.13	0.14	0.15	0.17	0.18	0.14	0.15	0.15	0.15	0.02
LOI	18.66	17.76	19.35	20.54	17.91	20.74	17.13	21.52	17.97	21.74	17.19	20.77	20.79	22.29	21.69	21.94	22.27	22.47	21.69	23.34	20.95	21.9	21.60	22.62	21.63	22.03	0.61
Total	100.00	100.00	100.00	100.00	100.00	100.00	100.00	100.00	100.00	100.00	100.00	100.00	100.00	100.00	100.00	100.00	100.00	100.00	100.00	100.00	100.00	100.00	100.00	100.00	100.00	100.0	0.00
CaO*	0.01	0.01	0.01	0.01	0.01	0.01	0.02	0.01	0.01	0.01	0.01	0.01	0.01	0.01	0.01	0.01	0.01	0.01	0.01	0.01	0.01	0.01	0.01	0.01	0.01	0.01	0.00
CIA	83.04	81.57	84.08	82.84	82.43	83.76	82.60	84.03	85.42	84.14	84.11	85.56	85.84	84.97	85.12	85.09	82.41	82.91	86.10	86.09	82.40	84.00	84.55	84.29	83.15	84.26	1.31
PIA	92.39	92.26	93.66	93.23	92.51	93.12	91.97	93.18	93.42	93.23	93.45	93.98	94.36	94.55	94.64	94.43	93.10	93.36	94.99	95.35	93.00	94.25	94.31	94.20	93.48	94.14	0.75
CIW	93.33	93.38	94.44	94.16	93.52	93.96	92.98	93.98	94.09	94.03	94.24	94.62	94.96	95.20	95.28	95.08	94.08	94.27	95.54	95.88	93.98	95.01	95.01	94.93	94.36	94.89	0.59
ICV	1.14	1.19	0.92	1.21	1.15	1.14	1.08	1.18	1.08	1.17	1.14	1.07	1.04	1.12	1.13	1.03	1.21	1.09	1.04	1.13	1.15	1.23	1.13	1.14	1.21	1.13	0.06
Al_2O_3/Na_2O	14.22	14.33	17.25	16.38	14.67	15.80	13.45	15.88	16.17	16.00	16.63	17.88	19.14	20.17	20.50	19.64	16.14	16.71	21.78	23.62	15.88	19.33	19.37	19.03	17.00	18.86	7.28
K_2O/Na_2O	1.89	2.22	2.25	2.38	2.11	2.05	1.82	2.00	1.74	2.00	2.13	2.00	2.14	2.55	2.57	2.42	2.43	2.43	2.50	2.80	2.38	2.67	2.52	2.53	2.43	2.52	0.12
SiO_2/Al_2O_3	7.43	6.87	8.67	10.34	10.81	9.20	8.15	10.37	9.08	10.00	8.51	9.03	9.70	7.83	7.98	7.74	5.52	5.05	10.12	9.49	6.31	6.45	7.51	6.97	6.90	7.32	1.47

$(SiO_2)_{adj}$ = major element data were recalculated to anhydrous (LOI-free) basis and adjusted to 100%; Fe_2O_3* total Fe expressed as Fe_2O_3; CIA = $[Al_2O_3 / (Al_2O_3 + CaO^* + Na_2O + K_2O)] \times 100$ (Nesbitt and Young 1982); PIA = $[(Al_2O_3 - K_2O) / (Al_2O_3 + CaO^* + Na_2O)] \times 100$ (Fedo et al. 1995); CIW = $[Al_2O_3 / (Al_2O_3 + CaO^* + Na_2O)] \times 100$ (Harnois 1988); CaO* CaO in silicate phase. To calculate CaO*, the assumption proposed by McLennan et al. (1993) was followed. ICV = $(Fe_2O_3 + K_2O + Na_2O + CaO + MgO + MnO + TiO_2) / Al_2O_3$ (Cox et al. 1995)

n number, *std* standard deviation

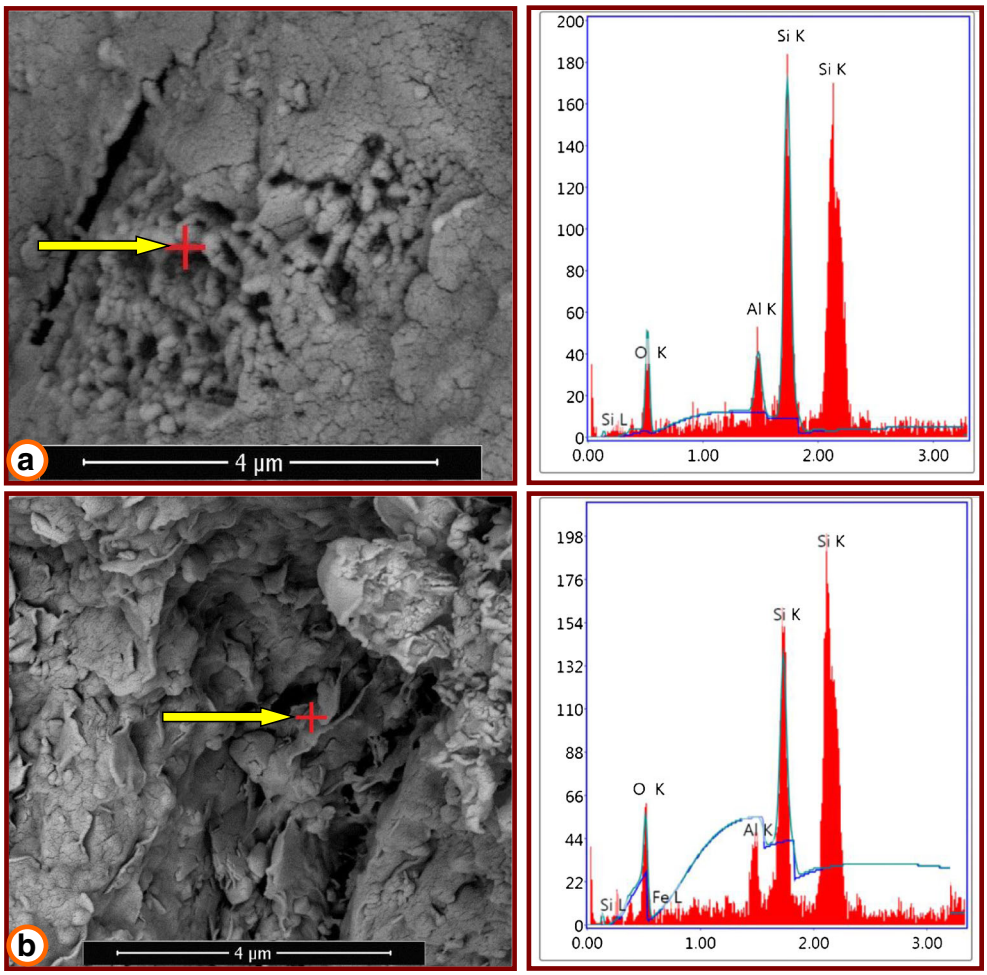

Fig. 5 SEM and EDS spectrum for the Duwi black shale samples. **a** El Sebaiya (sample US1). **b** Elgididh-6 (Eg5). Arrow mark shows the points where the EDS analyses were performed

(Table 1). The presence of pyrite in shales indicates the prevalence of a reducing environment during deposition. The reduction of sea water sulfate bacterial activity leads to pyrite formation in sediments (Berner 1982).

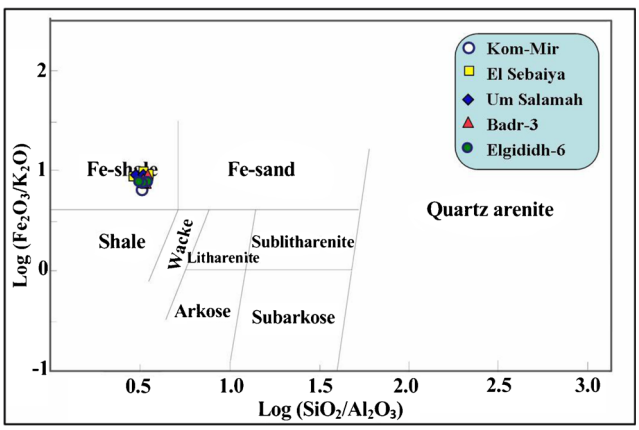

Fig. 6 Geochemical classification diagram using log (SiO_2/Al_2O_3)–log (Fe_2O_3/K_2O) (after Herron 1988)

Major and trace element concentrations

The major element concentrations of the black shales of the Upper Cretaceous Duwi Formation are reported in Table 2. SiO_2 is the dominant constituent of the Duwi black shales in all studied sites (avg. = 41.69%, Table 2). Al_2O_3 (avg. = 12.12%) and $Fe_2O_3^t$ (avg. = 10.93%) are the second abundant elements in studied samples. The SiO_2/Al_2O_3 ratios vary from 5.05 and 10.8 (avg. = 7.32) higher than that for pure kaolinite (1.18) and smectite (2.81–3.31). This indicates that the shales consist mainly of a mixture of smectite and kaolinite. Cao (avg. = 5.89%) and P_2O_5 (avg. = 2.83%) are the third abundant elements in shale samples (Table 2). The average values of Cao and P_2O_5 are relatively comparable to the average marine black shales of Nile Valley (Temraz 2005). The shale samples are less abundant in K_2O and MgO contents and are depleted in Na_2O, TiO_2, and SO_3. Depletion of Na_2O in shales suggests either lesser amount of plagioclase detritus in the shales and/or comparatively intense chemical weathering at the source and during fluvial

Table 3 Trace element composition (ppm) of the studied samples

Location	Kom-Mir					El Sebaiya					Um Salamah					Badr-3					Elgididh-6					Av	Std
	KM1	KM2	KM3	KM4	KM5	Sb1	Sb2	Sb3	Sb4	Sb5	US1	US2	US3	US4	US5	B1	B2	B3	B4	B5	Eg1	Eg2	Eg3	Eg4	Eg5		
Sr	251	422	561	1597	277	1200	704	208	351	493	411	860	811.67	1025	660	953	129	644	891	1031	76	300	474	484	513	613	365
Ba	256	333	132	211	139	362	225	88	104	120	240	225	161	237	242	111	109	99	53	88	93	33	73	78	91	156	88
V	191	199	244	200	255	158	157	155	258	260	211	214	233	204	190	121	156	1452	209	412	111	144	377	3050	2677	474	766
Ni	29	39	31	35	38	32	31	32	29	32	30	35	25	32	31	30	30	147	38	60	81	48	126	188	154	55.3	46.3
Co	5	4	5	5	4	6	4	5	4	5	5	4	5	5	4	5	5	12	7	8	16	9	18	18	19	7.5	4.9
Cr	74	99	108	94	105	64	57	50	112	174	94	100	102	88	75	35	122	540	100	240	81	28	177	630	412	150	152
Zn	71	99	43	42	66	65	53	40	61	82	71	61	50	58	61	40	133	1041	121	63	69	36	1246	1600	1110	255	452
Cu	26	31	21	21	51	10	10	9	22	34	26	24	31	27	24	9	24	156	10	33	27	9	156	243	177	48	62
Zr	299	344	234	374	221	40	40	40	70	100	292	317	276	212	100	39	144	106	41	54	138	39	109	93	98	153	110
Cs	1.0	8.0	7.0	6.0	7.0	1.0	4.0	7.0	7.5	8.0	5.0	7.0	7.0	5.0	4.0	1.0	0.0	1.0	0.0	0.0	7.0	1.0	8.0	7.0	7.0	4.7	3.0
Cd	3.0	0.0	1.0	4.0	7.0	4.0	4.0	4.0	2.5	1.0	1.0	2.0	4.0	5.0	5.0	0.0	4.0	4.0	7.0	0.0	1.0	0.0	4.0	7.0	7.0	3.3	2.3
Mo	3.0	4.0	4.0	1.0	5.0	4.0	4.0	4.0	4.0	4.0	4.0	3.0	3.0	3.0	4.0	1.0	4.0	30.0	4.0	4.0	4.0	9.0	21.0	7.0	25.0	6.5	7.4
U	14.0	5.0	5.0	4.0	7.0	51.0	27.5	4.0	4.5	5.0	5.0	5.0	4.0	20.0	28.0	24.0	9.0	44.0	27.0	11.0	4.0	27.0	52.0	41.0	34.0	18.5	16.0
Th	18.0	10.0	10.0	9.0	14.0	1.0	5.0	9.0	9.5	10.0	10.0	10.0	11.0	8.0	5.0	1.0	10.0	9.0	1.0	10.0	9	1	8	9	8	8.2	4.0
Pb	14.0	63.0	15.0	13.0	12.0	14.0	13.5	13.0	13.5	14.0	31.0	30.0	13.0	13.0	13.0	13.0	12.0	30.0	15.0	13.0	14	15	33	20	29	19.2	11.5
Sc	7.0	5.0	7.0	8.0	5.0	9.0	10.5	12.0	9.5	7.0	6.0	7.0	7.0	7.0	8.0	11.0	10.0	7.5	6.6	8.5	8.0	12.0	13.0	8.0	9.0	8.3	2.1
Hf	1.2	1.4	1.5	1.2	1.4	1.2	1.2	1.3	1.3	1.3	1.6	1.7	1.3	1.5	1.3	2.0	1.8	1.7	1.2	1.6	1.0	1.2	1.6	1.3	1.5	1.4	0.2
Rb	28.0	29.0	44.0	41.0	46.0	9.0	9.5	10.0	22.5	35.0	34.0	38.0	60.0	48.0	38.0	10.0	33.0	41.0	10.0	19.0	28	10	32	31	30	29.4	14.1
La	24.6	26.5	7.3	25.4	11.2	30.0	18.6	14.3	30.2	16.3	9.6	17.2	0.1	10.3	3.0	19.1	34.3	0.2	20.6	6.0	17.7	21.9	8.7	10.4	8.2	8.3	2.1
Rb/Sr	0.11	0.07	0.08	0.03	0.17	0.01	0.01	0.05	0.06	0.07	0.08	0.04	0.07	0.05	0.06	0.01	0.26	0.06	0.01	0.02	0.37	0.03	0.07	0.06	0.06	0.1	0.1
Cr/Ni	2.55	2.54	3.48	2.69	2.76	2.00	1.84	1.56	3.86	5.44	3.13	2.86	4.08	2.75	2.42	1.17	4.07	3.67	2.63	4.00	1.00	0.58	1.40	3.35	2.68	2.7	1.1
La/Sc	3.51	5.29	1.04	3.18	2.23	3.33	1.77	1.19	3.18	2.33	3.51	3.51	0.01	1.47	0.38	1.74	3.43	0.03	3.12	0.71	2.21	3.51	3.51	1.29	0.91	8.3	2.1
La/Co	4.91	6.61	1.45	5.08	2.79	5.00	4.65	2.86	7.55	3.26	2.73	2.73	0.02	1.14	0.38	3.82	6.86	0.02	2.94	0.75	1.11	2.73	2.73	0.58	0.91	8.3	2.1
Th/Sc	2.57	2.00	1.43	1.13	2.80	0.11	0.48	0.75	1.00	1.43	1.67	1.43	1.57	1.14	0.63	0.09	1.00	1.20	0.15	1.18	1.13	0.08	0.62	1.13	0.89	1.1	0.7
Th/Co	3.60	2.50	2.00	1.80	3.50	0.17	1.25	1.80	2.38	2.00	2.00	2.50	2.20	1.60	1.25	0.20	2.00	0.75	0.14	1.25	0.56	0.11	0.44	0.50	0.42	1.5	1.0
Cr/Th	4.11	9.90	10.80	10.44	7.50	64.00	11.40	5.56	11.79	17.40	9.40	10.00	9.27	11.00	15.00	35.00	12.20	60.00	100.00	24.00	9.00	28.00	22.13	70.00	51.50	24.8	24.9
Ni/Co	5.80	9.75	6.20	7.00	9.50	5.33	7.75	6.40	7.25	6.40	6.00	8.75	5.00	6.40	7.75	6.00	6.00	12.25	5.43	7.50	5.06	5.33	7.00	10.44	8.11	7.1	1.8
V/Cr	2.58	2.01	2.26	2.13	2.43	2.47	2.75	3.10	2.30	1.49	2.24	2.14	2.28	2.32	2.53	3.46	1.28	2.69	2.09	1.72	1.37	5.14	2.13	4.84	6.50	2.7	1.2

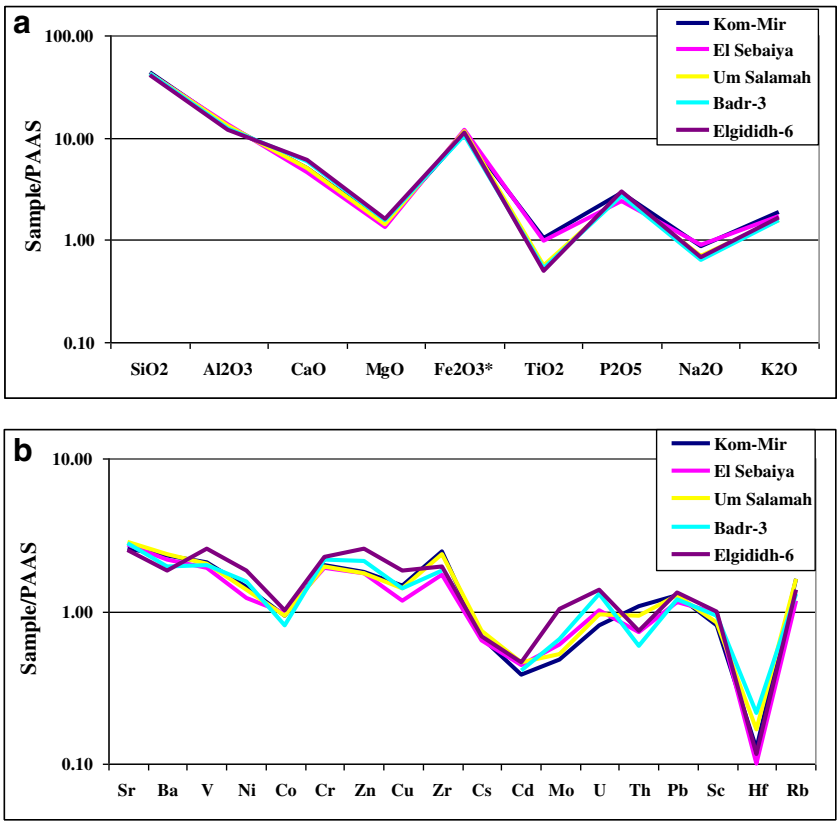

Fig. 7 Distribution of PAAS normalized abundance of Duwi black shales. **a** Major elements. **b** Trace elements

transportation of the detrital material of the shales. Depletion of TiO_2 and low K_2O content indicates the presence of relatively lesser quantities of phyllosilicate minerals in the shales (McCann 1991; Condie et al. 1992; Armstrong-Altrin 2015). The SEM-EDS study reveals that the Duwi black shale samples are rich in Si, Al, K, and Fe contents, which may suggest the abundance of quartz and clay minerals (Fig. 5). On the SiO_2/Al_2O_3 versus Fe_2O_3/K_2O geochemical classification diagram, the shale samples are classified mainly as Fe-shale (Fig. 6; Herron 1988), which is also consistent with the petrographic data.

The trace element concentrations of the Upper Cretaceous Duwi black shales for the five investigated sites are listed in Table 3. Figure 7a, b shows the distribution of major and selected trace element contents of the shales normalized to PAAS (Post Archaean Australian Shale; Taylor and McLennan 1985). Compared to PAAS, the Upper Cretaceous Duwi black shales are highly enriched in SiO_2, Al_2O_3, CaO, Fe_2O_3, P_2O_5, Sr, Ba, V, Ni, Cr, Zn, Cu, and Rb and slightly enriched in MgO, K_2O, U, Th, and Cd and Sc, Zr, Pb, and Co contents and highly depleted in TiO_2, Na_2O, Hf, and Cs content. The similar trace element content in shales may be related to the same source rock compositions. Strontium is the most abundant trace element in the studied samples (average = 600 ppm). The high Sr content may be due to the presence of aragonitic fossils and shells. Vanadium is the second abundant trace element in black shale samples. The concentration of V (avg. = 376 ppm) is more than those of Turekian and Wedepohl (1961) and Vine and Tourtelot (1970) may be due to oxidation and weathering of the organic matter. Zinc is the third abundant trace element in studied shales (255 ppm). The studied Duwi black shale samples also contain high concentrations of Cr, Ba, Zr, Cu, and Ni (158, 156, 153, 48, and 47 ppm, respectively). This enrichment is due to the contribution by intermediate and mafic source rocks.

The positive correlation between Al_2O_3 and SiO_2, TiO_2, and Zr ($r = 0.59$, 0.69, and 0.55, respectively, $n = 25$, Table 4) can be explained by a terrigenous origin. This may be due to the presence of a considerable amount of detrital clays. There is a weak positive correlation between Fe_2O_3 and the SiO_2, Al_2O_3, MgO, TiO_2, Na_2O ($r = 0.18$, 0.15, 0.17, 0.21, and 0.55, respectively, Table 4) and a significant correlation between Fe_2O_3 and Ni ($r = 0.82$). This may be due to the association of Fe^{3+} with clay minerals. K_2O shows a positive correlation with SiO_2, Al_2O_3, and TiO_2 ($r = 0.51$, 0.30, and 0.49, respectively). This indicates the association of K_2O with aluminosilicate phases.

Table 4 Values of Pearson's coefficient of correlation of major and trace elements in Duwi black shales

	SiO_2	Al_2O_3	CaO	MgO	Fe_2O_3	TiO_2	P_2O_5	Na_2O	K_2O	Sr	Ba	V	Ni	Co	Cr	Zn	Cu	Zr	Cs	Cd	Mo	U	Th	Pb	Sc	Hf	Rb
SiO_2	1																										
Al_2O_3	0.599	1																									
CaO	−0.500	−0.567	1																								
MgO	−0.116	−0.450	0.226	1																							
Fe_2O_3	0.182	0.150	−0.370	0.171	1																						
TiO_2	0.621	0.687	−0.403	−0.393	0.211	1																					
P_2O_5	−0.362	−0.556	0.455	0.250	−0.345	−0.335	1																				
Na_2O	0.353	0.478	−0.131	−0.368	0.552	0.649	−0.284	1																			
K_2O	0.519	0.307	0.179	−0.123	0.206	0.491	−0.039	0.748	1																		
Sr	−0.074	0.376	−0.384	−0.276	−0.022	0.038	−0.398	−0.185	−0.113	1																	
Ba	0.201	0.512	−0.140	−0.375	0.318	0.469	−0.212	0.502	0.430	0.318	1																
V	−0.254	−0.296	0.378	0.126	−0.288	−0.278	0.018	−0.223	−0.069	−0.087	−0.285	1															
Ni	−0.261	−0.365	0.509	0.173	0.828	−0.342	0.018	−0.306	−0.102	−0.130	−0.352	0.866	1														
Co	−0.314	−0.126	0.329	−0.076	0.181	−0.110	0.185	0.259	0.392	−0.278	−0.071	−0.003	−0.012	1													
Cr	−0.235	−0.309	0.427	0.141	−0.453	−0.319	−0.049	−0.340	−0.181	−0.047	−0.372	0.855	0.980	−0.095	1												
Zn	−0.263	−0.318	0.439	0.132	−0.370	−0.332	0.012	−0.304	−0.122	−0.105	−0.357	0.845	0.956	−0.010	0.943	1											
Cu	−0.214	−0.311	0.415	0.189	−0.372	−0.312	0.008	−0.286	0.156	−0.132	−0.335	0.892	0.974	−0.037	0.960	0.982	1										
Zr	0.300	0.553	−0.069	−0.217	0.750	0.253	0.169	0.276	0.351	0.087	0.504	−0.159	−0.152	−0.022	−0.176	−0.204	−0.126	1									
Cs	0.290	0.244	−0.280	−0.266	0.128	0.277	−0.030	0.264	0.182	−0.236	0.002	0.158	0.139	0.096	0.131	0.180	0.241	0.356	1								
Cd	0.048	−0.042	−0.062	0.216	−0.071	−0.153	−0.302	−0.121	−0.065	0.051	−0.108	0.501	0.395	−0.020	0.392	0.464	0.476	−0.154	0.028	1							
Mo	−0.297	−0.305	0.555	0.111	−0.351	−0.346	0.057	−0.220	−0.033	−0.147	−0.348	0.580	0.799	0.095	0.729	0.751	0.724	−0.236	0.000	0.285	1						
U	−0.358	−0.123	0.333	0.156	−0.216	−0.311	−0.176	−0.271	−0.110	0.202	−0.062	0.446	0.561	0.004	0.543	0.661	0.571	−0.521	−0.340	0.432	0.605	1					
Th	0.326	−0.084	0.024	0.091	0.048	0.191	0.178	0.282	0.130	−0.396	0.108	0.070	0.159	−0.117	0.146	0.038	0.148	0.615	0.390	−0.034	−0.015	−0.503	1				
Pb	0.057	0.117	0.355	−0.386	−0.180	0.203	0.081	0.115	0.294	−0.111	0.291	0.200	0.353	−0.059	0.282	0.321	0.313	0.374	0.310	−0.164	0.364	0.088	0.119	1			
Sc	−0.429	−0.416	0.121	0.038	0.154	−0.289	0.144	−0.180	−0.215	−0.047	−0.419	−0.024	0.041	−0.035	0.029	0.194	0.068	−0.623	−0.181	−0.064	0.222	0.395	−0.446	−0.245	1		
Hf	−0.076	−0.127	0.277	0.066	−0.398	−0.306	0.031	−0.313	−0.242	0.081	−0.117	0.073	0.207	−0.376	0.210	0.171	0.160	0.029	−0.187	−0.157	0.241	0.070	0.004	0.230	0.107	1	
Rb	0.344	0.172	−0.088	0.350	−0.174	−0.021	−0.029	0.061	0.168	−0.165	0.076	0.056	0.124	−0.046	0.111	0.037	0.166	0.558	0.416	0.284	0.051	−0.287	0.590	0.003	−0.573	0.096	1

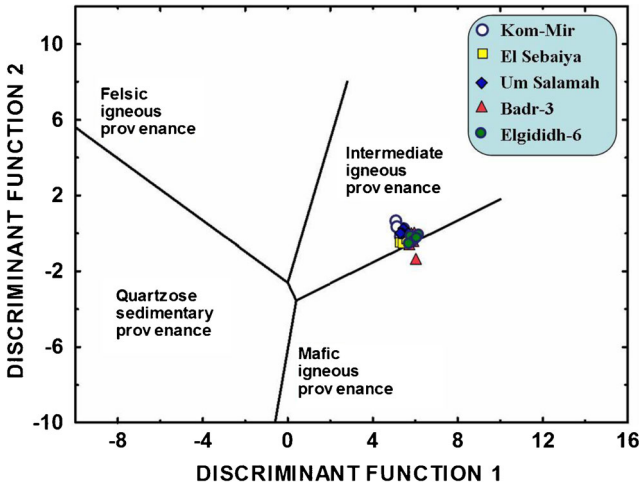

Fig. 8 Provenance discrimination diagram for shales (after Roser and Korsch 1988). Discriminant function 1 = (− 1.773 × TiO_2%) + (0.607 × Al_2O_3%) + (0.76 × $Fe_2O_3^T$%) + (− 1.5 × MgO%) + (0.616 × CaO%) + (0.509 × Na_2O%) + (− 1.22 × K_2O%) + (− 9.09). Discriminant function 2 = (0.445 × TiO_2%) + (0.07 × Al_2O3%) + (− 0.25 × $Fe_2O_3^T$%) + (− 1.142 × MgO%) + (0.438 × CaO%) + (0.432 × Na_2O%) + (1.426 × K_2O%) + (− 6.861)

Discussion

Source area weathering

The intensity and duration of weathering in clastic sediments can also be assessed by examining the relationship between alkali and alkaline earth elements (Nesbitt and Young 1982). The degree of weathering is quantified by various methods. The commonly used weathering indices like chemical index of alteration (CIA; Nesbitt and Young 1982), chemical index of weathering (CIW; Harnois 1988), and plagioclase index of alteration (PIA; Fedo et al. 1995) are widely used to deduce the intensity of the source area weathering (Armstrong-Altrin and Machain-Castillo 2016; Zaid 2017a, b; Abou El-Anwar et al. 2017). According to Fedo et al. (1995), the CIA, CIW, and PIA values of ~ 60 indicates low weathering, ~ 60–80 moderate weathering, and more than 80 indicate intensive weathering. The CIA values of the Upper Cretaceous Duwi black shales varies from 82 to 86% (avg. = 84%). The average CIA is higher than the PAAS values (70–75; Taylor and McLennan 1985), suggesting an intensive degree of chemical weathering in the source area. The PIA values range from 92 to 95% (avg. = 94%) indicating a high degree of alteration of source material. CIW values range from 93 to 96% (avg. = 95%) also indicate high degree of weathering. Based on CIA, PIA, and CIW values (> 80%), it can be concluded that the lithocomponents in shales were subjected to intense chemical weathering and reflect warm/humid climatic conditions in the depositional basin (McLennan et al. 1993).

The maturity of shale can be identified by the ratio values of SiO_2/Al_2O_3, Al_2O_3/Na_2O, and K_2O/Na_2O, which increase when maturity increases. The ratio values > 6, > 5, and < 0.5, respectively, may indicate high maturity of sediments (Cox et al. 1995). The SiO_2/Al_2O_3, Al_2O_3/Na_2O, and K_2O/Na_2O ratio values of the Duwi black shales in all studied sites (~ 5.0–10.8, ~ 13.4–23.6, and ~ 1.7–2.8, respectively) suggest moderate compositional maturity.

The index of compositional variability (ICV; Cox et al. 1995) is considered as an important parameter to evaluate the maturity of sediments (Cullers 2000). ICV values are high (> 1) for detrital ferromagnesian minerals and feldspars and low (< 1) for the clay minerals subjected to intensive weathering processes (Cox et al. 1995; Cullers 2000). The ICV values of the Duwi black shales range from 0.92 to 1.23% (average = 1.13 ± 0.06, n = 25) are slightly more than 1 (Table 2), indicating the presence of detrital ferromagnesian minerals beside the abundant clay minerals. Compositionally submature to mature sediments with slightly high ICV values are partially recycle deposits derived by intensive weathering of source rocks (Zaid 2017a, b).

Table 5 Range of elemental ratios of Duwi black shales in this study compared to the ratios in similar fractions derived from felsic, mafic rocks, and upper continental crust

Elemental ratio	Kom-Mir[a]	El Sebaiya[a]	Um Salamah[a]	Badr-3[a]	Elgididh-6[a]	Range of sediment from felsic sources[b]	Range of sediment from mafic sources[b]	UCC[c]
La/Sc	3.05	2.36	3.07	1.80	3.0	2.50–16.3	0.43–0.86	2.21
La/Co	2.21	2.34	2.21	2.76	2.21	1.80–13.8	0.14–0.38	1.76
Th/Sc	1.99	0.75	1.29	0.72	0.77	0.84–20.5	0.05–0.22	0.79
Th/Co	1.42	0.76	1.02	2.41	0.72	0.67–19.4	0.04–1.40	0.63
Cr /Th	8.55	22.03	10.93	46.24	41.13	4.00–15.0	25–500	7.76

[a] This study

[b] Cullers (1994, 2000), Cullers and Podkovyrov (2000)

[c] Taylor and McLennan (1985)

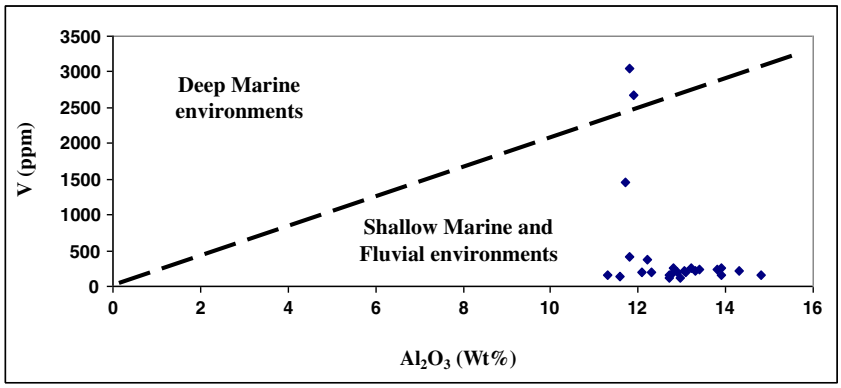

Fig. 9 Plot of V versus Al_2O_3 in the Duwi black shales for paleoenvironmental reconstructions

Provenance

The chemical analyses of the clastic sediments has been widely used to identify the source rock characteristics (Armstrong-Altrin et al. 2015a, b; Abou El-Anwar and Gomaa 2016; Zaid 2017a, b). In order to infer the provenance of siliclastic rocks, several major and trace element-based discrimination diagrams have been proposed by many investigators (Roser and Korsch 1988; Floyd et al. 1989; McLennan et al. 1993; Verma and Armstrong-Altrin 2013, 2016; Verma et al. 2016). On the major element-based provenance discrimination diagram of Roser and Korsch (1988), the studied Upper Cretaceous Duwi black shales plot exclusively in the quartzose sedimentary provenance fields (Fig. 8). The Al_2O_3/TiO_2 ratio and SiO_2 contents can be used to identify the source rock (Hayashi et al. 1997). The Al_2O_3/TiO_2 ratio of the Duwi black shales vary from 9.92 to 49.6 (avg. 23.6), and SiO_{2adj} contents vary from 51.0 to 55.7 wt% (avg. 53.47 wt%). These values suggest that the source rocks for the shales are intermediate and mafic igneous rocks. K_2O/Na_2O ratio can be considered as a simplified chemical provenance indicator (Potter 1978). The K_2O/Na_2O ratio (avg. = 2.52, Table 2) reflects derivation from intermediate or basic rocks.

The concentration of the transition trace elements can be used to identify the composition of the source rocks (Garver et al. 1996; Armstrong-Altrin 2009). The studied samples have higher contents of some transition metals such as V, Zn, and Cr (average of 376, 255, and 158 ppm, respectively) and slightly depleted in some others such as Cu, Ni, and Co (average of 48, 47, and 9 ppm, respectively) compared with PAAS. Figure 7 indicates that the source area was dominated by rocks of intermediate type with subordinate of mafic composition. The positive correlation between Cr and Ni ($r = 0.98$, Table 4) and the Cr/Ni ratios (3.86) revealed that few mafic components from the basement source rocks accumulated during weathering. They are probably derived from the basement terrains in the Red Sea Hills and transported via Wadi el-Shaghab and Wadi el-Miyah (Fig. 1).

The trace element ratios such as La/Sc, La/Co, Th/Sc, Th/Co, and Cr/Th values of the Upper Cretaceous Duwi black shale are compared in Table 5, with those of sediments derived from mafic and felsic source rocks (Cullers 1994, 2000; Cullers and Podkovyrov 2000; Taylor and McLennan 1985). These ratios of the studied shale samples fall within the range of sediments derived mainly from intermediate and mafic igneous source rocks (Table 5). The Precambrian gabbro and metagabbro–diorite complex could have been the main source rocks with subordinate recycled Upper Cretaceous Nubia Formation for Duwi black shales.

Depositional environment

The chemical analysis data can be used to evaluate the paleo-redox conditions of siliciclastic rocks during sedimentation (Armstrong-Altrin et al. 2015a; Armstrong-Altrin and Machain-Castillo 2016). The high enrichment of Sr, V, Ni, Cr, Zn, and Cd in the investigated Duwi black shale samples is comparable with those values of modern black shales directly due to mafic input. The average value of Fe_2O_3/TiO_2 ratio is 21.42, which is consistent with mafic input as well (Abou El-Anwar et al. 2017). In addition, the V–Al_2O_3 and P_2O_5–Al_2O_3 bivariate diagrams can be used to discriminate depositional environments of shales. The V–Al_2O_3 bivariate plot (Fig. 9) shows that most of studied shale samples plot on shallow marine depositional environments.

The Ni/Co ratio values can be used as an indicator for paleo-redox conditions. The values of Ni/Co ratios below 5 indicate oxic environments, whereas values of this ratio above 5 suggest suboxic and anoxic depositional environments (Jones and Manning 1994). Ni/Co ratio of the studied black shales varies from 5.0 to 12.25 (avg. = 7.1, Table 3) suggest that the deposition of these shales is performed under suboxic and anoxic conditions. The values of V/Cr ratios are also considered as an indicator of paleo-redox conditions. The V/Cr ratio values ranges from 1.28 to 6.5 (avg. = 2.7, Table 3) which revealed that it was deposited under anoxic conditions (Hallberg 1976). The average value of Mo/Al_2O_3 ratios of the investigated samples is 0.5, which is slightly higher than the PAAS shale standard value (0.1; Taylor and

McLennan 1985), suggest anoxic conditions for studied shales. Such conditions can only result from anaerobic bacterial activity.

Conclusions

The Duwi black shales are classified mainly as Fe-shale. Compared to PAAS, the shales are highly enriched in SiO_2, Al_2O_3, CaO, Fe_2O_3, and P_2O_5 and highly depleted in TiO_2 and Na_2O content. The positive correlation between Al_2O_3 and SiO_2, TiO_2, and Zr indicate a considerable amount of detrital clays. K_2O shows a positive correlation with both SiO_2 and Al_2O_3, which indicates the association of K_2O with aluminosilicate phases.

The CIA, CIW, and PIA values of the Duwi black shales suggest recycle deposits and intensive weathering in the source region and reflect warm/humid climatic conditions in the depositional basin. The SiO_2/Al_2O_3, Al_2O_3/Na_2O, and K_2O/Na_2O ratio values of the Duwi black shales in all studied sites suggest moderate compositional maturity. The ICV values of the Duwi black shales (avg. = 1.13) are slightly more than 1, indicating the presence of detrital ferromagnesian minerals beside the abundant clay minerals.

The geochemistry results indicate that the Duwi black shales were mainly derived from the Precambrian gabbro and metagabbro–diorite complex with subordinate recycled sedimentary rocks (Nubia Formation). The Fe_2O_3/TiO_2, Ni/Co, V/Cr, and Mo/Al_2O_3 ratio values and the high concentration of Sr, V, Ni, Cr, Zn, and Cd in the investigated Duwi black shales indicate that the shales were deposited under anoxic reducing marine environments.

Acknowledgements The author thanks members of the laboratory of the Central Metallurgical Research and Development Institute, Egypt, for facilitating analytical work for the present research. Thanks also to the journal reviewers, for their very constructive and helpful comments as well as for editorial comments, which helped to improve the manuscript.

References

Abou El-Anwar EA, Gomaa MM (2016) Electrical, mineralogical, geochemical and provenance of Cretaceous black shales, Red Sea Coast, Egypt. Egypt J Pet 25:323–332

Abou El-Anwar EA, Mekky HS, Abd El Rahim SH, Aita SK (2017) Mineralogical, geochemical characteristics and origin of Late Cretaceous phosphorite in Duwi Formation (Geble Duwi Mine), Red Sea region, Egypt. Egypt J Pet 26:157–169

Armstrong-Altrin JS (2009) Provenance of sands from Cazones, Acapulco, and Bahía Kino beaches, Mexico. Rev Mex Cienc Geol 26:764–782

Armstrong-Altrin JS (2015) Evaluation of two multi-dimensional discrimination diagrams from beach and deep sea sediments from the Gulf of Mexico and their application to Precambrian clastic sedimentary rocks. Int Geol Rev 57:1446–1461

Armstrong-Altrin JS, Machain-Castillo ML (2016) Mineralogy, geochemistry, and radiocarbon ages of deep sea sediments from the Gulf of Mexico, Mexico. J S Am Earth Sci 71:182–200

Armstrong-Altrin JS, Lee YI, Verma SP, Ramasamy S (2004) Geochemistry of sandstones from the Upper Miocene Kudankulam Formation, southern India: implications for provenance, weathering, and tectonic setting. J Sediment Res 74:285–297

Armstrong-Altrin JS, Nagarajan R, Madhavaraju J, Rosales-Hoz L, Lee YI, Balaram V, Cruz-Martinez A, Avila-Ramirez G (2013) Geochemistry of the Jurassic and upper Cretaceous shales from the Molango Region, Hidalgo, eastern Mexico: implications for source-area weathering, provenance, and tectonic setting. Compt Rendus Geosci 345(4):185–202

Armstrong-Altrin JS, Machain-Castillo ML, Rosales-Hoz L, Carranza-Edwards A, Sanchez-Cabeza JA, Ruíz-Fernández AC (2015a) Provenance and depositional history of continental slope sediments in the Southwestern Gulf of Mexico unraveled by geochemical analysis. Cont Shelf Res 95:15–26

Armstrong-Altrin JS, Nagarajan R, Balaram V, Natalhy-Pineda O (2015b) Petrography and geochemistry of sands from the Chachalacas and Veracruz beach areas, western Gulf of Mexico, Mexico: constraints on provenance and tectonic setting. J S Am Earth Sci 64:199–216

Basu A, Bickford ME, Deasy R (2016) Inferring tectonic provenance of siliciclastic rocks from their chemical compositions: a dissent. Sediment Geol 336:26–35

Berner RA (1982) Burial of organic carbon and pyrite sulfur in the modern ocean: its geochemical and environmental significance. Am J Sci 282:451–473

Bhatia MR (1985) Rare earth element geochemistry of Australian Paleozoic graywackes and mudrocks: provenance and tectonic control. Sediment Geol 45:97–113

Borghesi F, Migani F, Dinelli E (2016) Geochemical characterization of surface sediments from the northern Adriatic wetlands around the Po River delta. Part II: aqua regia results. J Geochem Explor 169:13–29

Bottcher ME, Hetzel A, Brumsack HI, Schipper A (2006) Sulfur-iron-carbon geochemistry in sediments of the Demerara Rise. Proc ODP Sci Results 207:1–23

Campodonico VA, García MG, Pasquini AI (2016) The geochemical signature of suspended sediments in the Parana River basin: implications for provenance, weathering and sedimentary recycling. Catena 143:201–214

Condie KC, Boryta MD, Liu J, Quian X (1992) The origin of khondalites: geochemical evidence from the Archean to Early Proterozoic granulite belt in the North China craton. Precambrian Res 59:207–223

Conoco (1987) Geological map of Egypt, scale (1:500,000), NG 36 SE Gebel Hamata

Cox R, Lowe DR, Cullers RL (1995) The influence of sediment recycling and basement composition on evolution of mudrock chemistry in the southwestern United States. Geochim Cosmochim Acta 59: 2919–2940

Cullers RL (1994) The controls on the major and trace element variation of shales, siltstones, and sandstones of Pennsylvanian-Permian age from uplifted continental blocks in Colorado to platform sediment in Kansas, USA. Geochim Cosmochim Acta 58:4955–4972

Cullers RL (2000) The geochemistry of shales, siltstones and sandstones of Pennsylvanian-Permian age, Colorado, U.S.A.: implications for provenance and metamorphic studies. Lithos 51:181–203

Cullers RL, Podkovyrov VN (2000) Geochemistry of the Mesoproterozoic Lakhanda shales in southeastern Yakutia, Russia: implications for mineralogical and provenance control, and recycling. Precambrian Res 104:77–93

Davis JC (1986) Statistics and data analysis in geology. Wiley, Hoboken 646p

El Kammar MM (1993) Organic and inorganic components of the Upper Cretaceous-Lower Tertiary black shales from Egypt and their hydrocarbon potentialities. Ph.D.Thesis, Cairo Univ., Egypt

El Kammar AM (2014) Oil shale resources in Egypt: the present status and future vision. Arab Geo-Front 1:1–34

El Kammar AM, Darwish M, Phillip G, El Kammar MM (1990) Composition and origin of black shales from Quseir area, Red Sea coast, Egypt. J Univ Kuwait (Sci) 17:177–190

El-Azabi MH, Farouk S (2010) High resolution sequence stratigraphy of the Massstrichtian—Ypresian succession along the eastern scarp face of Kharga Oasis, southern Western Desert, Egypt. Sedimentology:1–35

Fedo CM, Nesbitt HW, Young GM (1995) Unraveling the effects of Kmetasomatism in sedimentary rocks and paleosols with implications for palaeoweathering conditions and provenance. J Geol 23: 921–924

Floyd PA, Franke W, Shail R, Dorr W (1989) Geochemistry and tectonic setting of Lewisian clastic metasediments from the Early Proterozoic Loch Maree Group of Gairloch, NW Scotland. Precambrian Res 45: 203–214

Garver JI, Royce PR, Smick TA (1996) Chromium and nickel in shale of the Taconic Foreland: a case study for the provenance of fine-grained sediments with an ultramafic source. J Sediment Res 66: 100–106

Ghandour IM, Harue M, Wataru M (2003) Mineralogical and chemical characteristics of Bajocian-Bathonian shales, G. Al-Maghara, North Sinai, Egypt: climatic and environmental significance. Geochem J 37:87–108

Ghanem MF, El-Fakharany MA, Temraz MG, Afife MM, Shehata AM (2016) Mineralogical and elemental compositions of oil shale in Duwi Formation phosphate mines, Safaga-Quseir Egypt. Int J Innov Sci Eng Technol 3(2):479–493

Glenn CR, Arthur MA (1990) Anatomy and origin of a Cretaceous phosphorite-Green sand giant, Egypt. Sedimentology 37:123–154

Hallam A, Grose JA, Ruffell AH (1991) Paleoclimatic significance of changes in clay mineralogy across the Jurassic-Cretaceous boundary in England and France. Palaeogeogr Palaeoclimatol Palaeoecol 81: 173–187

Hallberg RO (1976) A geochemical method for investigation of paleoredox conditions in sediments. Ambient Species Rep 4:139–147

Hardy R, Tucker M (1988) X-ray powder diffraction of sediments. In: Tucker M (ed) Techniques in sedimentology. Blackwell, Cambridge, pp 191–228

Harnois L (1988) The CIW index: a new chemical index of weathering. Sediment Geol 55(3–4):319–322

Hayashi KI, Fujisawa H, Holland HD, Ohomoto H (1997) Geochemistry of ~1.9 Ga sedimentary rocks from northern Labrador, Canada. Geochim Cosmochim Acta 61(19):4115–4137

Heath R, Vanstone S, Swallow J, Ayyad M, Amin M, Huggins P, Swift R, Warburton I, McClay K, Younis A (1998) Renewed exploration in the off shore north Red Sea region, Egypt. Proceedings of the 14th petroleum conference, Egyptian General Petroleum Corporation, Cairo, Egypt: 16–34

Hendriks F, Luger P, Strouhal A (1990) Early tertiarymarine palygorskite and sepiolite neoformation in SE Egypt. Z Deut Geol Ges 141:87–97

Herron MM (1988) Geochemical classification of terrigenous sands and shales from core or log data. J Sediment Petrol 58:820–829

Ibrahim DM, Abdel Aziz DA, Awad SA, Abdel Monem AM (2004) Utilization of black shales in earthware recipes. Ceram Int 30(6): 829–835

Jones B, Manning DC (1994) Comparison of geochemical indices used for the interpretation of paleo-redox conditions in Ancient mudstones. Chem Geol 111(1–4):111–129

Khalil SM, McCLay KR (2009) Structural control syn-rift sedimentation, north west Red Sea margin, Egypt. Mar Pet Geol 26:1018–1034

Loukola-Ruskeeniemi K (1991) Geochemical evidence for a hydrothermal origin of sulphur, base metals and gold in Phanerozoic metamorphosed black shales, Kainuu and Outokumpu areas, Finland. Mineral Deposita 26:152–164

McCann T (1991) Petrological and geochemical determination of provenance in the southern Welsh Basin. In: Morton AC, Todd SP, Haughton PDW (eds) Developments in Sedimentary Provenance Studies, vol. 57. Geol Soc London, Spec Publ, 215–230

McLennan SM, Hemming S, McDaniel DK, Hanson GN, (1993) Geochemical approaches to sedimentation, provenance, and tectonics. In: Johnsson MJ, Basu A (eds) Processes controlling the composition of clastic sediments: J Geol Soc America, special paper, 21–40

Mondal MEA, Wani H, Mondal B (2012) Geochemical signature of provenance, tectonics and chemical weathering in the quaternary flood plain sediments of the Hindon River, Gangetic plain, India. Tectonophysics 566–7:87–94

Moore DM, Reynolds RC Jr (1997) X-ray diffraction and the identification and analysis of clay minerals. Oxford University Press, New York 378p

Nagarajan R, Madhavaraju J, Nagendra R, Armstrong-Altrin JS, Moutte J (2007) Geochemistry of Neoproterozoic shales of the Rabanpalli formation, Bhima Basin, northern Karnataka, southern India: implications for provenance and paleoredox conditions. Rev Mex Cienc Geológicas 24(2):150–160

Nesbitt HW, Young GM (1982) Early Proterozoic climates and plate motions inferred from major element chemistry of lutites. Nature 299:715–717

Ollier CD, Galloway RW (1990) The laterite profile ferricrete and unconformity, vol 17. Canda Verlag, Cremlingen, pp 97–109

Pettijohn FJ (1975) Sedimentary rocks, 3rd edn. Harper and Row, New York 628p

Potter PE (1978) Petrology and chemistry of modern big river sands. J Geol 86:423–449

Roser BP, Korsch RJ (1988) Provenance signatures of sandstone-mudstone suites determined using discrimination function analysis of major element data. Chem Geol 67:119–139

Said R (1990) The geology of Egypt. A.A. Balkema, Rotterdam 734p

Said R (1992) The geology of Egypt. Elsevier Science Ltd., Rotterdam

Schulte P, Scheibner C, Speijer RP (2011) Fluvial discharge and sea-level changes controlling black shale deposition during the Paleocene–Eocene thermal maximum in the Dababiya quarry section, Egypt. Chem Geol 285:167–183

Schulte P, Schwark L, Stassen P, Tanja JK, Bornemann A, Speijer RP (2013) Black shale formation during the Latest Danian Event and the Paleocene–Eocene Thermal Maximum in central Egypt: two of a kind? Palaeogeogr Palaeoclimatol Palaeoecol 371:9–25

Schultz RB (1991) Geochemical characterization of black shale types in the Midcontinent Pennsylvanian. PhD dissertation. Univ. Cincinnati, Ohio, 229

Sediek KN, Amer AM (2001) Sedimentological and technological studies of Abu Tartur black shales, Western Desert, Egypt. Physicochem Probl Miner Process 35:141–152

Selley RC (1988) Applied Sedimentology. - Textbook. 446p

Selvaraj K, Lin BZ, Lou J-Y, Xia WL, Huang XT, Chen C-TA (2016) Lacustrine sedimentological and geochemical records for the last 170 years of climate and environmental changes in southeastern China. Boreas 45:165–179

Tawfik HA, Ghandour IM, Maejima W, Armstrong-Altrin JS, Abdel-Hameed A-MT (2016) Petrography and geochemistry of the siliciclastic Araba Formation (Cambrian), east Sinai, Egypt: implications for provenance, tectonic setting and source weathering. Geol Mag. https://doi.org/10.1017/S0016756815000771

Taylor SR, McLennan SM (1985) The continental crust: its composition and evolution. Blackwell, Oxford

Temraz MA (2005) Mineralogical and geochemical studies of carbonaceous shale deposits from Egypt. Ph.D. Thesis, Berlin Uni. Berlin., Germany

Tobia FH, Shangola SS (2016) Mineralogy, geochemistry and depositional environment of the Beduh Shale (Lower Triassic), Northern Thrust Zone, Iraq. Turk J Earth Sci 25:367–391

Turekian KK, Wedepohl KH (1961) Distribution of the elements in some major units of the earth's crust. Bull Geol Soc Am 72:175–192

Verma SP, Armstrong-Altrin JS (2013) New multi-dimensional diagrams for tectonic discrimination of siliciclastic sediments and their application to Precambrian basins. Chem Geol 355:117–180

Verma SP, Armstrong-Altrin JS (2016) Geochemical discrimination of siliciclastic sediments from active and passive margin settings. Sediment Geol 332:1–12

Verma SP, Díaz-González L, Armstrong-Altrin JS (2016) Application of a new computer program for tectonic discrimination of Cambrian to Holocene clastic sediments. Earth Sci Inf 9:151–165

Vine JD, Tourtelot EB (1970) Geochemistry of black shales a summary report. Econ Geol 65:253–273

Wignall PBZ (1993) Distinguishing between oxygen and subtract control in fossil benthic assemblages. J Geol Soc Lond 150:193–196

Zaid SM (2017a) Provenance of coastal dune sands along Red Sea, Egypt. J Earth Syst Sci 126(4):1–20

Zaid SM (2017b) Petrography and geochemistry of the Middle Miocene Gebel El Rusas sandstones, Eastern Desert, Egypt: implications for provenance and tectonic setting. J Earth Syst Sci 126(7):1–22